Coherent Nonlinear Optical Response of Single Quantum Dots Studied by Ultrafast Near-Field Spectroscopy

Tobias Guenther, Christoph Lienau, and Thomas Elsaesser
Max-Born-Institut für Nichtlineare Optik und Kurzzeitspektroskopie, D-12489 Berlin, Germany

Markus Glanemann, Vollrath Martin Axt, and Tilmann Kuhn
Institut für Festkörpertheorie, Universität Münster, D-48149 Münster, Germany

Soheyla Eshlaghi and Andreas D. Wieck
Lehrstuhl für Angewandte Festkörperphysik, Ruhr-Universität Bochum, D-44870 Bochum, Germany
(Received 21 February 2002; published 15 July 2002)

The nonlinear response of single GaAs quantum dots is studied in femtosecond near-field pump-probe experiments. At negative time delays, transient reflectivity spectra show pronounced oscillatory structure around the quantum dot exciton line, providing the first evidence for a perturbed free induction decay of the excitonic polarization. Phase-disturbing Coulomb interactions between the excitonic polarization and continuum excitations dominate the optical nonlinearity on ultrafast time scales. A theoretical analysis based on the semiconductor Bloch equations accounts for this behavior.

DOI: 10.1103/PhysRevLett.89.057401 PACS numbers: 78.67.Hc, 07.79.Fc, 78.47.+p

The study of single quantum systems such as trapped atoms or ions, single molecules, and nanostructures provides insight into the fundamental processes of light-matter interaction and is relevant for implementing new concepts of optical quantum information processing. Semiconductor quantum dots (QDs) with electronic wave functions localized on a nanometer length scale, atomiclike densities of states [1–3], and comparatively long dephasing times [4,5] represent important model systems for investigating coherent nonlinear optical phenomena, e.g., Rabi oscillations [6,7] or optical control of polarizations [8], and for realizing basic quantum optical functions [9–11], i.e., photon antibunching [12], one-qubit rotations [6], and optically induced entanglement [13].

An important prototype QD system is a thin semiconductor quantum well (QW), where local minima of the QW disorder potential caused by interface roughness and alloy fluctuations lead to the localization of excitons with a confinement energy on the order of 10 meV. The large extension of the exciton center-of-mass wave function in such ''interface'' QDs of 30–50 nm gives rise to large single QD dipole moments of 50 to 75 Debye [6]. The statistical distribution of localized wave functions and optical transition energies results in optical spectra which consist of a distribution of narrow lines, influenced by effects such as energy-level repulsion [14]. The excitonic lines display a homogeneous linewidth of 30–50 μeV, in agreement with measured dephasing times of 20–30 ps [8].

The nonlinear optical properties of excitons in single interface QDs have mainly been investigated by high-resolution nonlinear spectroscopy in the frequency domain [15]. The third-order nonlinear response has been explained on the basis of homogeneously broadened two-level systems, in analogy to descriptions of atomic systems. On the other hand, many-body effects mediated through Coulomb interaction play an important role for third-order nonlinearities in higher-dimensional semiconductor structures, i.e., quantum wells and wires. So far, the role of many-body effects in QDs is not understood. Transient Coulomb interactions arising from multiexcitonic excitations [11] and/or nonresonant optical excitations of the QD and its environment (e.g., neighboring QDs [10]) should also affect QD optical nonlinearities and their ultrafast dynamics. Such couplings are difficult to probe and/or control in studies of QD ensembles, making time-resolved studies of single QDs desirable.

In this Letter, we report the first femtosecond study of the nonlinear optical response of a single QD. After nonresonant femtosecond excitation of carriers in continuum states, we observe, unlike in atomic systems, transient differential reflectivity spectra with pronounced oscillatory structures around the QD exciton resonance. These oscillations persist up to negative delay times of more than 10 ps and reflect the perturbation of the free induction decay of the coherent QD polarization by transient many-body interactions.

We investigate interface QDs in a 5.1 nm thick GaAs QW layer grown by molecular beam epitaxy between two AlAs/GaAs superlattice barriers on a (100) GaAs substrate and buried 120 nm below the sample surface. The growth was interrupted at the two interfaces to ensure a large correlation length of the disorder potential and to form interface QDs.

A near-field scanning optical microscope [16] operating at 10 K is used in a pump-probe setup [17] with a combined spatial and temporal resolution of 200 nm and 150 fs, respectively [Fig. 1(a)]. Collinearly polarized pump and probe pulses are derived from a 30 fs Ti-sapphire oscillator,

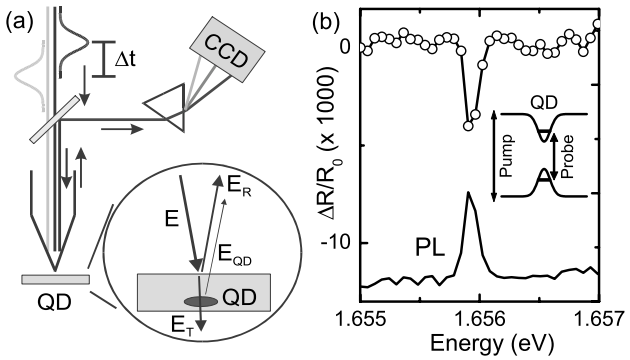

FIG. 1. (a) Schematic of the experimental setup. (b) Near-field PL spectrum of a single QD (solid line) and differential reflectivity $\Delta R/R_0$ at $\Delta t = 30$ ps. PL and ΔR are recorded with identical pump pulses centered at 1.675 eV, exciting electron-hole pairs in 2D continuum states. Inset: schematic energy diagram.

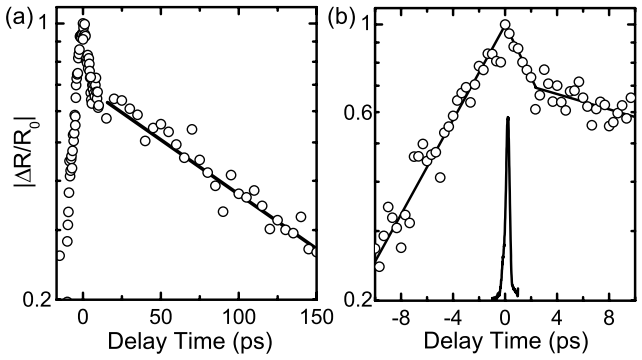

FIG. 2. (a) Time evolution of $\Delta R(E_{\mathrm{QD}})/R_0$ for a single QD resonance at $E_{\mathrm{QD}} = 1.6598$ eV (logarithmic ordinate scale). The decay is biexponential with a slow decay time 150 ps. (b) Early time dynamics of $\Delta R(E_{\mathrm{QD}})/R_0$. A slow rise of $\Delta R/R_0$ is observed at negative delay times. Solid line around delay zero: cross correlation of pump and probe pulses indicating a time resolution of 150 fs.

spectrally and temporally shaped and coupled into a chemically etched, uncoated near-field fiber probe. Photoluminescence (PL) from the sample and/or the reflected probe light are collected through the same fiber, dispersed in a $f = 50$ cm monochromator, and detected with a cooled charge-coupled device (CCD) with a resolution of 60 μeV. The pump pulses at 1.675 eV (power 120 nW) create about five electron-hole pairs per pulse in QW continuum states, corresponding to an excitation density of 5×10^9 cm^{-2}. Spectral shaping ensures that resonant QD excitation is negligible. The 100 nW probe pulses of 18 meV bandwidth are centered at 1.655 eV, around the QW absorption resonance. Differential probe reflectivity spectra $\Delta R(E_{\mathrm{det}}, \Delta t)/R_0 = [R(E_{\mathrm{det}}, \Delta t) - R_0(E_{\mathrm{det}})]/R_0(E_{\mathrm{det}})$ are recorded at a fixed spatial position of the near-field tip as a function of the time delay Δt between pump and probe pulses [$R_0(E_{\mathrm{det}})$: steady state reflectivity at a photon energy E_{det}].

Far-field QW PL spectra show a 5 meV inhomogeneously broadened line centered at 1.658 eV that breaks up into a series of spectrally sharp emission lines when recorded with high spatial/spectral resolution [3,14,18]. These emission lines originate from excitons localized in individual interface QDs [14]. After fs excitation at 1.675 eV, five to ten emission lines are resolved in the near-field PL spectrum. For delay times $\Delta t > 0$, differential reflectivity spectra measured with the same pump power of 120 nW display spectrally sharp resonances at the same spectral position, E_{QD}, as the simultaneously recorded PL lines [Fig. 1(b)]. The linewidth of PL and ΔR is mainly limited by the monochromator resolution. For pump and probe powers of up to 250 nW, $\Delta R(E_{\mathrm{QD}})$ varies linearly with pump and probe intensity, respectively.

Figure 2(a) displays the time evolution of the spectrally resolved reflectivity change measured on the QD resonance at 1.6598 eV (circles). After a picosecond rise of the signal at negative delay times, one finds a fast partial decay with a time constant of about 6 ps, followed by a much slower decay with a time constant of 150 ps. The fast signal components are very similar for different QDs investigated, whereas the decay time of the slow component varies between 30 and 150 ps. Such time constants are determined by radiative recombination in the QDs [3] and will be discussed elsewhere. In Fig. 2(b), the early time dynamics of $\Delta R(E_{\mathrm{QD}}/R_0)$ is plotted on an extended scale. The 8 ps rise of the signal occurs much slower than the 150 fs cross correlation of pump and probe pulses. The reflectivity $\Delta R_t(\Delta t) = \int dE_{\mathrm{det}}\, \Delta R(E_{\mathrm{det}}, \Delta t)$ integrated over an interval of 2 meV around E_{QD} (not shown) vanishes for $\Delta t < 0$ and shows the slow exponential decay at $\Delta t > 0$.

The spectral characteristics of $\Delta R/R_0$ are markedly different at positive and negative Δt (Fig. 3). At $\Delta t < 0$, pronounced *spectrally symmetric* oscillations around the excitonic resonance are observed. Their oscillation period decreases with increasing negative delay. At $\Delta t > 0$, the spectra show a bleaching of the QD resonance.

We now consider the origin of the transient signals observed in reflection. As shown schematically in Fig. 1(a), the reflected probe field, locally collected by the near-field tip, represents a superposition of the field $E_R(t)$ reflected from the sample surface, and the field $E_{\mathrm{QD}}(t)$, radiated in back-direction from the probe-induced excitonic polarization $P_{\mathrm{QD}}(t) = \int dt'\, \chi_{\mathrm{QD}}(t') E_T(t - t')$ of the QD, located 120 nm below the surface. Here, $E_T(t)$ and χ_{QD} denote the probe field interacting with the QD and the QD susceptibility, respectively. The time-integrated reflectivity $R_0(\omega)$ detected behind the monochromator is proportional to $|\tilde{E}_{\mathrm{QD}}(\omega) + \tilde{E}_R(\omega)|^2$, where $\tilde{}$ denotes the Fourier transform. Excitation by the pump pulse affects the QD polarization and, thus, results in a change of reflectivity. For time delays $\Delta t < 0$, the pump pulse perturbs the free induction decay of the polarization created by the

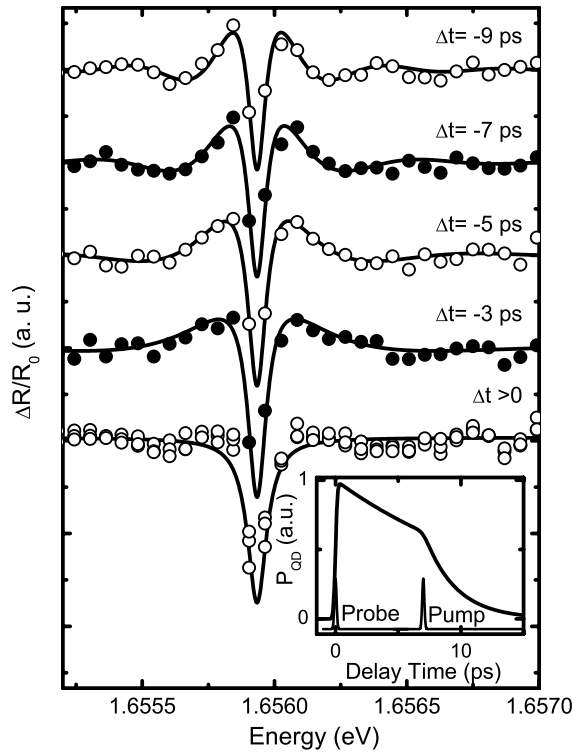

FIG. 3. Near-field $\Delta R/R_0$ spectra (circles) at different delay times Δt. The spectra at $\Delta t < 0$ display pronounced spectral oscillations around the excitonic resonance. The solid line shows simulated spectra for the perturbed free induction decay of the coherent QD polarization assuming $T_2 = 15$ ps. Inset: simulated dynamics of $P_{\mathrm{QD}}(t)$.

probe pulse (inset in Fig. 3). For $\Delta t > 0$, the probe interacts with the system modified by the pump, resulting in a probe polarization different from the unexcited system. The differential reflectivity $\Delta R(\omega, \Delta t)$ represents the spectral interferogram of $\tilde{E}_R$ and $\tilde{E}_{\mathrm{QD}}$:

$$\Delta R(\omega, \Delta t) \propto \mathrm{Re}\{\tilde{E}_R^*(\omega)[\tilde{E}_{\mathrm{QD}}(\omega, \Delta t) - \tilde{E}_{\mathrm{QD},0}(\omega)]\}. \quad (1)$$

Here the finite monochromator resolution and the weak contribution from $|\tilde{E}_{\mathrm{QD}}|^2$ have been neglected. The line shape of $\Delta R(\omega, \Delta t)$ evidently depends on the phase delay between $E_R(t)$ and $E_{\mathrm{QD}}(t)$. As a function of distance d between QD and surface, it oscillates between absorptive and dispersive shape. In our measurements, with $d = 120$ nm, this results in an absorptive (Lorentzian) line shape at $\Delta t \gg 0$ [19], and ΔR probes the imaginary part of the QD polarization, $\mathrm{Im}(P_{\mathrm{QD}})$. In the frequency domain, a perturbed free induction decay of the polarization induced by the probe pulse leads to oscillatory features in the spectrum $\Delta R(\omega, \Delta t)$ with a period determined by the time delay between probe and pump.

In our experiments, the pump pulse creates electron-hole pairs in QW states well above the QD resonance. The data in Figs. 2 and 3 provide the first direct evidence for a perturbed free induction decay of the excitonic QD polarization induced by this type of excitation. Both pronounced reflectivity changes at negative time delays (Fig. 2) and spectral oscillations depending on the pump-probe delay (Fig. 3) are observed. In general, pump-induced many-body interactions perturb the free induction decay of $P_{\mathrm{QD}}(t)$ by changing the resonance energy, oscillator strength, and/or dephasing rate of the QD polarization. Energy renormalizations give rise to spectrally asymmetric nonlinearities, as, e.g., for the dynamic Stark shift of exciton lines in QWs [20,21]. Such energy shifts are absent in our data displaying symmetric oscillatory features (Fig. 3). The spectrally integrated reflectivity change ΔR_t vanishes for each of the spectra recorded at negative time delays and, thus, changes of the oscillator strength are negligible. We conclude that the pump-induced damping of the QD polarization is the leading contribution to the QD nonlinearity at early times. Such excitation-induced dephasing (EID) [22] of the QD polarization arises from Coulomb scattering with the initial *nonequilibrium* carrier distribution in QW continuum states [23]. The damping time of the QD polarization after the arrival of the pump pulse determines the energy range over which the reflectivity spectra display oscillations. In Fig. 3, spectral oscillations are observed in a window of about 0.5 meV around the QD resonance, corresponding to a damping on a time scale of a few ps. The solid lines in Fig. 3 are calculated from a simple model in which the probe-induced QD polarization $P_{\mathrm{QD}}(t)$ decays initially with an effective dephasing time $T_2 = 15$ ps decreasing to $T_{\mathrm{EID}} = 3$ ps after the arrival of the pump laser (inset in Fig. 3). Because of the finite monochromator resolution, T_2 is a lower limit of the QD dephasing time $T_2(\mathrm{QD})$. The rise of $\Delta R(E_{\mathrm{QD}})$ at $\Delta t < 0$ is given by $T_2(\mathrm{QD})$ and the monochromator resolution. The measured rise of 8 ps is consistent with the deduced T_2 of 15 ps when the spectral resolution of 60 μeV per CCD pixel and the exact position of E_{QD} are taken into account.

A comment should be made on the reflectivity changes at positive time delays. Here carriers generated in continuum states by the pump pulse relax to low energy states in the QW disorder potential, among them the QD ground state. Relaxation to the QD ground state results in a Pauli blocking of the exciton transition and a concomitant change of reflectivity. The fast partial decay of $\Delta R(E_{\mathrm{QD}})/R_0$ in Fig. 2 reflects this redistribution process, whereas the subsequent slow decay is due to radiative recombination.

To confirm our qualitative interpretation, we analyze the nonlinear optical QD response on the basis of the semiconductor Bloch equations in mean-field approximation, including both disorder and Coulomb interaction. Nonlinear absorption spectra $\Delta A(\omega) \propto \mathrm{Im}[\tilde{E}_T^*(\omega)\tilde{P}(\omega)]$ are calculated, probing the imaginary part of P_{QD}, as in the experiment. We chose a one-dimensional Gaussian-correlated two-band disorder potential with a correlation length of 10 nm and a disorder strength of 5 meV [Fig. 4(a),

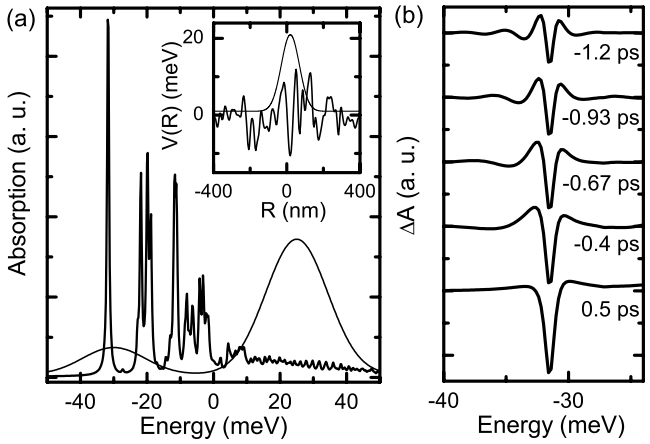

FIG. 4. (a) Spatially resolved linear absorption spectra of a QD ensemble calculated from the semiconductor Bloch equations. A Gaussian-correlated one-dimensional disorder potential is assumed (inset). Dashed lines: spectra of pump (centered at 25 meV) and probe pulses (at −30 meV). (b) Nonlinear absorption spectra for different pump-probe delays showing the perturbed free induction decay on the lowest resonance of (a).

inset]. Excitation-induced dephasing is treated phenomenologically [22] by a dephasing rate $\gamma = 1/T_2 + \gamma_1 n$ depending on the excitation density n. To reduce the numerical effort, the relevant dephasing rates have been scaled to $T_2(\mathrm{QD}) = 2$ ps, and γ_1 is chosen to yield a total dephasing time of $\gamma^{-1} \approx 0.4$ ps after the pulses. Pump and probe pulses are spatially localized to 100 nm. The linear absorption spectra show resonances from single localized excitons at low energies. Nonlinear absorption changes are calculated for 100 fs pump and probe pulses with the spectra shown in Fig. 4(a). The transient nonlinear absorption spectra [Fig. 4(b)] resolve the excitonic optical nonlinearity of a single QD. As in the experiment, transient spectral oscillations govern the optical nonlinearity at negative delay times. They are symmetrically centered around the exciton resonance and their oscillation frequency increases with time delay. When spectrally integrated, the QD nonlinearity vanishes at $\Delta t < 0$, indicating the importance of coherent contributions to the QD nonlinearity. $\Delta A(E_{\mathrm{QD}})$ rises at negative time delays with the time constant T_2. Neglecting EID, spectrally dispersive (asymmetric) line shapes are calculated in mean-field approximation, reflecting coherent renormalizations of the QD resonance energy. Such renormalizations obviously play a minor role if a continuum of states is excited in the surrounding of the QD. The theoretical simulations show clearly the importance of EID contributions to the perturbed free induction decay. Although single QDs resemble in many respects atomic systems, Coulomb many-body effects give rise to pronounced transient optical nonlinearities at negative delay times which have been reported so far only for higher-dimensional systems.

In conclusion, we have presented the first observation of the femtosecond excitonic nonlinearity of a single quantum dot. The free induction decay of the coherent excitonic polarization is perturbed by many-body interactions with continuum excitations on picosecond time scales. This opens the way to a controlled ultrafast manipulation of coherent quantum dot polarizations by external electromagnetic fields and/or material polarizations which is important for semiconductor-based implementation of quantum information processing.

We gratefully acknowledge support by the Deutsche Forschungsgemeinschaft (SFB296, SFB491), BMBF (01BM908/6), and the European Union through the EFRE and SQID programs.

[1] K. Brunner *et al.*, Phys. Rev. Lett. **73**, 1138 (1994).
[2] H. F. Hess *et al.*, Science **264**, 1740 (1994).
[3] D. Gammon *et al.*, Phys. Rev. Lett. **76**, 3005 (1996).
[4] P. Borri *et al.*, Phys. Rev. Lett. **87**, 157401 (2001).
[5] D. Birkedal, K. Leosson, and J. M. Hvam, Phys. Rev. Lett. **87**, 227401 (2001).
[6] T. H. Stievater *et al.*, Phys. Rev. Lett. **87**, 133603 (2001).
[7] H. Kamada *et al.*, Phys. Rev. Lett. **87**, 246401 (2001).
[8] N. H. Bonadeo *et al.*, Science **282**, 1473 (1998).
[9] A. Imamoğlu *et al.*, Phys. Rev. Lett. **83**, 4204 (1999).
[10] E. Biolatti *et al.*, Phys. Rev. Lett. **85**, 5647 (2000).
[11] P. Chen, C. Piermarocchi, and L. J. Sham, Phys. Rev. Lett. **87**, 067401 (2001).
[12] P. Michler *et al.*, Nature (London) **406**, 968 (2000).
[13] G. Chen *et al.*, Science **289**, 1906 (2000).
[14] F. Intonti *et al.*, Phys. Rev. Lett. **87**, 076801 (2001).
[15] N. H. Bonadeo *et al.*, Phys. Rev. Lett. **81**, 2759 (1998).
[16] A. Richter *et al.*, Phys. Rev. Lett. **79**, 2145 (1997).
[17] T. Guenther *et al.*, Appl. Phys. Lett. **75**, 3500 (1999).
[18] F. Intonti *et al.*, Phys. Rev. B **63**, 075313 (2001).
[19] The applicability of Eq. (1) has been validated by probing $\Delta R(\omega, \Delta t > 0)$ of single QDs buried at different depths d between the QW layer and the surface. These data (to be published) show the predicted transition between absorptive (Lorentzian) and dispersive line shapes.
[20] A. Mysyrowicz *et al.*, Phys. Rev. Lett. **56**, 2748 (1986).
[21] W. H. Knox *et al.*, Phys. Rev. Lett. **62**, 1189 (1989).
[22] H. Wang *et al.*, Phys. Rev. Lett. **71**, 1261 (1993).
[23] S. T. Cundiff *et al.*, Phys. Rev. Lett. **77**, 1107 (1996).